Journal of Population Therapeutics & Clinical Pharmacology

Hydrazone Ligand and Metal Complexes: A Comprehensive Study on Synthesis, Characterization, and Urease Inhibition Potential

Ghazali Hussain [1], Shumaila Akram [1], Mehreen Lateef [2], *Asad Khan Tanoli [1], Nida Ali [1] Zahid Khan [3]

[1]Department of Chemistry, Faculty of Science, University of Karachi, Pakistan
[2]Multidisciplinary Research Lab, Medical and Dental College, Bahria University, Karachi, 75500, Pakistan,
[3]Department of Chemistry, Faculty of Sciences, University of Swabi, Pakistan

Corresponding Author

*Asad Khan Tanoli [1], asad.tanoli@uok.edu.pk

ABSTRACT

This investigation delved into the imine group of hydrazones, elucidating its role in biological systems and emphasizing bioactivity and stable metal complexes vital for coordination chemistry. The main goal was to synthesize a hydrazone ligand, specifically 2-hydroxybenzaldehyde-N-(6-chloro-2-oxo-1,2-dihydro-3H-indol-3-ylidene), abbreviated as AG-41, along with its associated metal complexes utilizing Co(II), Ni(II), Cu(II), and Zn(II) ions. The newly synthesized compounds underwent comprehensive characterization, with a focus on revealing their structures and evaluating urease inhibition activity. The research aimed to identify novel metal complexes, employing hydrazone as ligands, which were synthesized and thoroughly characterized using various analytical techniques, including FT-IR, EI-mass, elemental analysis, UV-Visible, magnetic susceptibility, and conductivity studies. It was observed that in all cases, the ligand AG-41 exhibited tridentate coordination with the metal center. The ultimate goal was to contribute to understanding the structural determinants influencing urease inhibition, laying the groundwork for innovative urease inhibitors with potential applications in medical and

industrial domains. Results indicated that the metal complexes showed moderate potency, they were less effective in comparison to the hydrazone ligand. Importantly, both the ligand AG-41 and its precursor AG-40 displayed outstanding inhibitory properties when compared to the standard molecule i.e. Thiourea.

1 Introduction

The synthesis and exploration of chemical compounds with bioactive properties stand as fundamental pillars in scientific research, holding promise for addressing diverse challenges in both medical and industrial domains [1]. Within this context, the development of urease inhibitors has emerged as a focal point, garnering significant attention due to their relevance in various pathological conditions and industrial applications [2].

Urease, an enzyme dependent on nickel and prevalent in bacteria, fungi, and plants, plays a pivotal role in catalysing the hydrolysis of urea into ammonia and carbon dioxide [3]. Elevated urease activity poses health risks, contributing to urea-splitting urinary tract infections and urolithiasis [4]. Beyond health concerns, urease-induced corrosion impacts industries such as agriculture, petroleum, and wastewater treatment. In a biological context, urease's ability to raise pH by producing NH_3 influences medical conditions like kidney stones and bacterial infections [5]. Notably, Helicobacter pylori employs urease to survive acidic stomach conditions, leading to gastrointestinal issues. Targeting urease with inhibitors proves crucial for both medical intervention and industrial applications [6].

Hydrazones, characterized by the general structure $R_1R_2C=NR_3$, rank among the most widely utilized organic compounds. Serving various purposes, including pigments, dyes, catalysts, and intermediates in organic synthesis, they also exhibit diverse biological activities [7]. These activities span antifungal, antibacterial, antitumor, anti-inflammatory, anti-HIV, antimalarial, and anti-urease properties [8]. The distinctive imine group (-C=N-N=C-) in hydrazones facilitates comprehension of transamination and racemization reactions in biological systems [9].

Offering straightforward synthesis, stability, and diverse configurations, hydrazones play roles in materials, acid-degradable polymers for drug delivery, and exhibit valuable ligand properties in sensing technologies, biology, and catalysis. Particularly noteworthy is their role as potent anti-urease agents, with hydrazone derivatives demonstrating significant urease inhibition. Notably, those with a meta-positioned electron-withdrawing group (NO_2) exhibit the highest potency. Several hydrazones have been identified as effective urease inhibitors [10].

The ongoing research endeavors to delve into the potential of hydrazones and their metal complexes as urease inhibitors, aiming to unravel structural determinants influencing bioactivity. This exploration promises a novel approach to addressing urease-related issues, bridging the gap between fundamental scientific inquiry and practical applications in clinical pharmacology [11].

2 Methodology

2.1 Synthesis of Hydrazone Ligand

The synthesis of the ligand compound involved a two-step process. In the initial step, 0.02 mol of 6-chloro-isatin was introduced into a 50 mL beaker containing 20.0 mL of a hydrazine hydrated solution, with continuous stirring. The resulting reaction mixture was subsequently transferred to a 250 mL round bottom flask containing 50 mL of hot methanol. The flask was placed on a sand bath and refluxed for approximately one hour, yielding a yellow solid identified as "isatin monohydrazone." Following reflux, the flask was allowed to cool, and the solid product was filtered, successively washed, vacuum-dried, and subjected to recrystallization using methanol [12].

In the second step, a 0.04 mmol solution of 2-hydroxy-6-methoxybenzaldehyde in 10.0 mL of methanol was added to a 0.04 mmol solution of isatin monohydrazone in 50 mL of hot methanol. The resulting mixture was transferred to a 250 mL round bottom flask and refluxed on a sand bath for an additional 3 hours. Over time, a bright orange-colored product began to separate in the flask, and the progression of the reaction was monitored using thin-layer chromatography (TLC). Upon completion of the reaction, the flask was allowed to cool, and the solid product was filtered, washed, vacuum-dried, and recrystallized from methanol. Both steps of the synthesis yielded high quantities of the desired compound. Figure-1, represent the synthesis of hydrazone ligand [13].

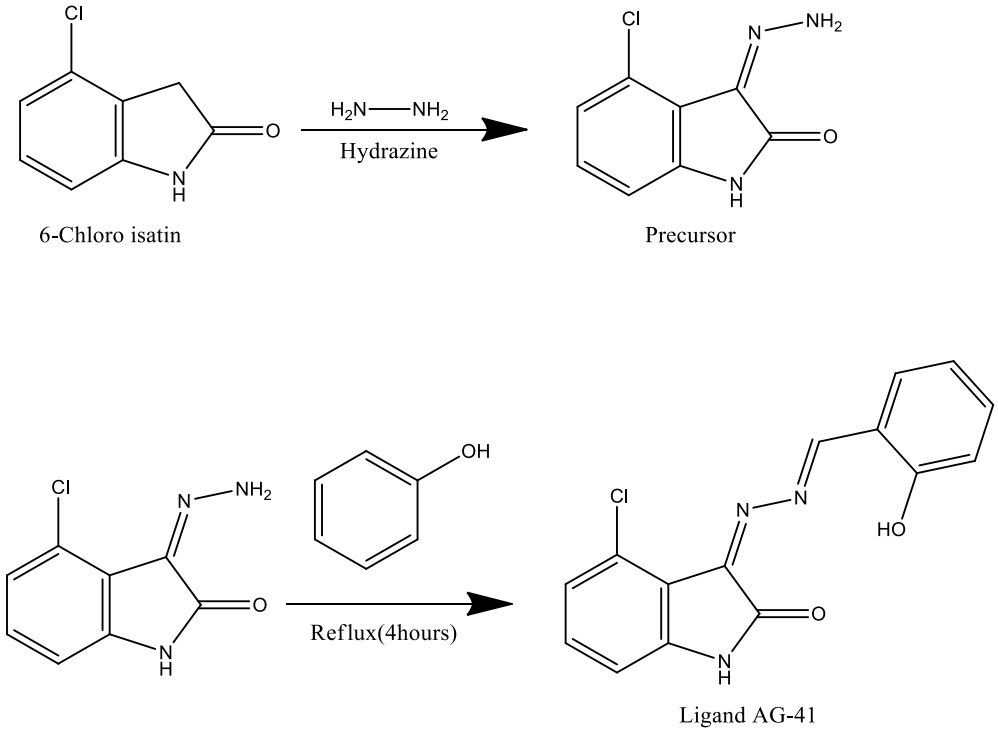

Figure-1 Synthesis of Hydrazone Ligand AG-41

2.2 Synthesis of Metal Complexes

Metal complexes of Co^{+2}, Ni^{+2}, Cu^{+2} and Zn^{+2} using a hydrazone ligand by refluxing a 0.2M metal chloride solution and a 0.4M ligand solution in methanol for 2 hours on a steam bath. After refluxing, concentrate the solution, filter it, and wash with CCl_4. Microcrystalline powder of metal complexes can be obtained by allowing slow evaporation from a methanolic solution [14]. Figure-2, represent the proposed structure of the complexes. The provided equations illustrate the suggested synthesis route.

$MaCl_2$ + AG-41 ⟶ [Ma(AG-41)$_2$] **Ma = Co(II), Ni(II)**

$MbCl_2$ + AG-41 ⟶ [Mb(AG-41)Cl] **Mb = Cu(II), Zn(II)**

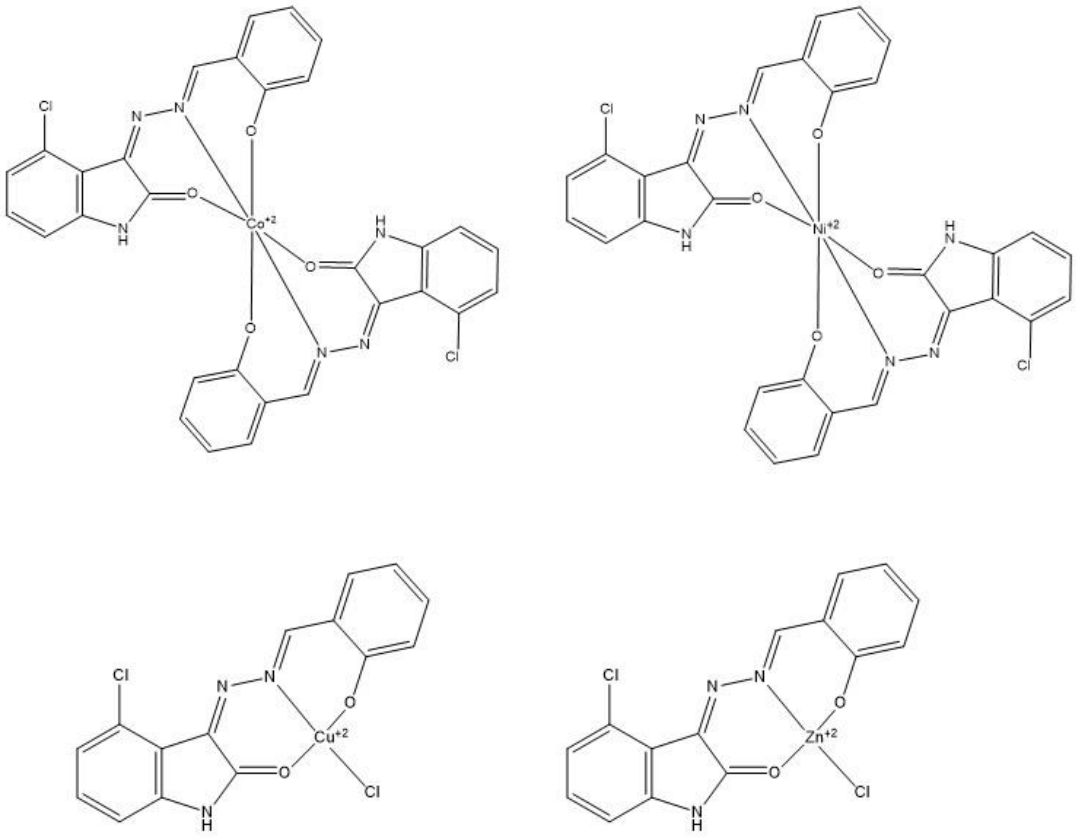

Figure-2 Proposed structures of the complexes

2.3 Urease inhibition assay

In 96-well plates, enzyme mixtures containing 25 µL of Jack bean urease solution and 55 µL of 100 mM urea buffers were incubated with 5 µL of test compounds (1 mM concentration) at 30 °C for 15 minutes. The determination of urease activity involved measuring ammonia production using the indophenol method as outlined by Weather burn. Specifically, 45 µL of phenol reagent (1% w/v phenol and 0.005% w/v sodium nitroprusside) and 70 µL of alkali reagent (0.5% w/v NaOH and 0.1% active chloride) were added. Each response was carried out three times. Thiourea was used as reference material and the following formula is used to calculate the percent inhibition [15].

Inhibition (%) = OD control - OD test comp/100 OD control

The inhibitor concentration (IC_{50}) at which an enzyme exhibits 50% inhibition. EZ-Fit 50 Enzyme Kinetics program measured these values.

3 Result and Discussion

3.1 Characterization of Metal Complexes

Metal complexes of hydrazone ligands in the solid state were characterized and purified through elemental analysis, including CHN, Infrared spectroscopy, proton NMR, Mass Spectroscopy, UV/Visible spectroscopy and conductivity measurements [16]. This data was utilized to deduce the precise coordination geometry around the metal in the solid state. All the complexes were identified as non-conductive, suggesting that the ligand AG-41 behaves as a tridentate ligand. Presented in table-1, are the physical and analytical data, which encompass CHN analysis.

Table-1 Physical and Analytical Analysis

Compounds		$C_{30}H_{18}Cl_2N_6O_4Co$	$C_{30}H_{18}Cl_2N_6O_4Ni$	$C_{15}H_9Cl_2N_3O_2Cu$	$C_{15}H_9Cl_2N_3O_2Zn$
Formula mass		656.349	656.11	397.708	399.55
Color		Crimson	Olive Green	Spruce	Tangerine
%Yield		63.5	61.2	56.1	69.6
M%	Observed	8.967	8.934	15.940	16.327
	Analyzed	*9.198*	*8.246*	*15.453*	*16.637*

C%	Observed	54.827	54.847	45.194	44.986
	Analyzed	*54.379*	*54.039*	*45.632*	*45.048*
H%	Observed	2.760	2.762	2.276	2.265
	Analyzed	*2.373*	*2.409*	*2.516*	*2.475*
N%	Observed	12.787	12.792	10.541	10.492
	Analyzed	*12.561*	*12.942*	*10.382*	*10.891*

3.2 Infrared Spectrum

The disappearance of the broad band at 3485 cm-^{1}, associated with the hydrogen-bonded OH group, in the infrared spectra of metal complexes suggests deprotonation and the formation of (C–O) bonds. A noticeable frequency increase (14 to 19 cm^{-1}) in (C-O) bonds indicates coordination of the phenolic oxygen to the metal ion. The stretching frequencies of (C=N) show a decrease of 19 to 42 cm^{-1} at 1558 cm^{-1}, supporting the involvement of aldimine nitrogen in coordination. The (C=O) band shifting to a lower frequency by 23 to 40 cm^{-1} in the metal complexes' spectra provides evidence for coordination by the carbonyl oxygen. However, the vibration characteristics of the ring (NH and C=N) remain unaltered, indicating their non-participation in coordination. Non-ligand peaks in the regions of 504–528 cm^{-1} and 427–445 cm^{-1} can be assigned to (M–O) and (M–N), respectively. Thus, the infrared spectra of the metal complexes clearly indicate coordination of the hydrazone ligand to the metal ions in a tridentate manner, involving the deprotonated phenolic oxygen, aldimine nitrogen, and carbonyl oxygen [17]. Figures 2 illustrate the proposed structures of the complexes. Table-2 provides the infrared spectral data along with possible assignments.

Table 2 Infrared spectral data of Hydrazone Ligand and Metal Complexes

Functional groups / assignments	**AG-41**	**[Co(AG-41)$_2$]**	**[Ni(AG-41)$_2$]**	**[Cu(AG-41)Cl]**	**[Zn(AG-41)Cl]**
υ (OH)	3485	3398	3416	3423	3437
υ NH	3263	3280	3276	3259	3290
υ C=O	1756	1732	1716	1730	1733
υ C≡N	1678	1683	1666	1690	1675
υ HC=N	1558	1516	1539	1523	1531

υ C-O	1366	1347	1383	1379	1350
υ N-N	1132	1147	1129	1114	1136
υ C-Cl	811	803	798	789	792
υ M-N		430	439	427	445
υ M-O		514	523	504	528

3.3 Electronic Spectra of Complexes

The electronic spectrum of the Co(II) complex exhibits absorption bands 16835 and 14245 cm^{-1}, corresponding to ^4T_1g (F) → ^4A_2g (F) and ^4T_1g (F) → ^4T_2g (F) transitions, respectively, within an octahedral environment. The lowest band, ^4T_1g (F) → ^4T_1g (P), remains unobservable due to limitations in the range of the instrument used. In the case of the Ni(II) complex, three absorption bands at 12048, 13986, and 24390 cm^{-1} are observed, associated with ^3A_2g → ^3T_2g; ^3A_2g → ^3T_1g (F) and ^3A_2g → ^3T_1g (P) transitions, respectively, within an octahedral environment. The electronic absorption spectra of Cu(II) complexes were recorded in methanol. Generally, ligand-related transitions manifest in the UV region, while d–d transitions occur in the visible domain. The Cu(II) complex spectra reveal absorption bands at 13423 and 24691 cm^{-1}. Studies attribute the intense high-energy band at 13698 cm^{-1} to the ligand-to-metal charge transfer (LMCT) transition. In concentrated solutions, a broad asymmetric band around 25000 cm^{-1}, assigned to d–d transitions (^2E_g → $^2T_{2g}$) for Cu(II) complexes with tetragonal distortion geometry due to the Jahn–Teller effect, is observed. Zn^{+2} complex displayed a singular absorption peak at approximately 26042cm^{-1}, indicating intra-ligand transitions. Due to d^{10} system, Zn^{+2} ion generally forms tetrahedral complexes. Notably, the Zn^{+2} complex didn't reveal any distinct d-d transitions and exhibited diamagnetic nature [18]. Table-3, represent the maximum wavelength i.e. λ max value of ligand and metal complexes.

Table 3 Electronic spectroscopic data of the hydrazone ligand and metal complexes

Compounds	**λ max nm /** wavenumber cm^{-1}		
AG-41	**268** / 37313	**315** / 31746	
$[Co(AG\text{-}41)_2]$	**594** / 16835	**702** / 14245	
$[Ni(AG\text{-}41)_2]$	**410** / 24390	**715** / 13986	**830** / 12048
[Cu(AG-41)Cl]	**405** / 24691	**745** / 13423	
[Zn(AG-41)Cl]	**384** / 26042		

Figure 3 Overlay Electronic Spectrum of Metal Complexes

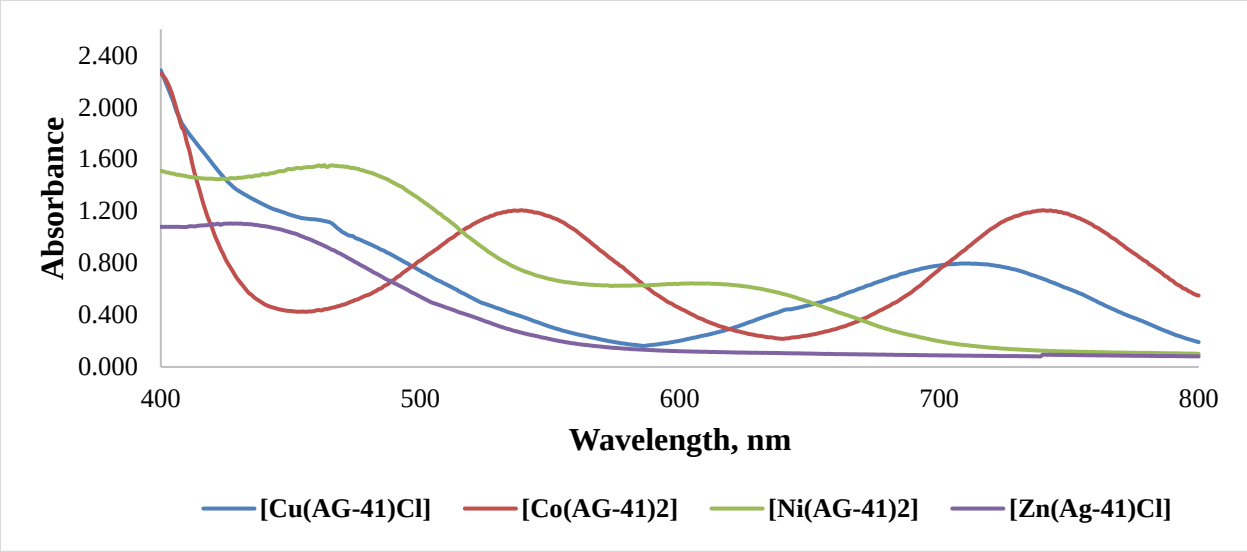

3.4 Urease Inhibition activity

The precursor AG-40 exhibits a notable urease inhibition activity with an inhibition of IC_{50} = 18.5±0.03. However, this inhibitory potential experiences a significant enhancement, reaching 26.7 ± 0.07, upon the formation of the corresponding ligand. This substantial increase in urease inhibition highlights the crucial role of the ligand in augmenting the inhibitory activity against urease. Table 4 showcases the IC_{50} values representing the urease inhibition activity of both the hydrazone ligand and metal complexes.

Table-4 IC_{50} values for Urease Inhibition activity of Hydrazone and metal complexes

Compound	IC_{50} (µM) Mean ± SEM
AG-40	18.5 ± 0.03
AG-41	26.7 ± 0.07
$[Co(AG\text{-}41)_2]$	59.8 ± 0.01
$[Ni(AG\text{-}41)_2]$	56.7 ± 0.13
[Cu(AG-41)Cl]	60.9 ± 0.11
[Zn(AG-41)Cl]	57.9 ± 0.05
Thiourea	21.5 ± 0.01

Surprisingly, a different turn when examining the urease inhibition activity of the metal complexes derived from the ligand. Contrary to the heightened inhibition observed with the ligand, the metal complexes display a decrease in urease inhibition activity, as evidenced by an increased IC_{50} value. This shift suggests that the introduction of metal ions alters the inhibitory efficacy against urease compared to the ligand alone.

Further analysis of the IC_{50} values for the metal complexes reveals a moderate inhibitory effect. This implies that while the metal complexes still retain some level of urease inhibition, it is not as potent as observed with the ligand alone. The contrast in inhibitory activity between the ligand and its metal complexes emphasizes the intricate relationship between the ligand structure and metal coordination in influencing the biological activity.

In comparison with the standard thioureas, the precursor i.e. monohydrazone molecule and the ligand AG-41 stands out as a promising urease inhibitor, showcasing a significant inhibitory avidity. This underlines the potential of the ligand as a valuable candidate for further exploration in the development of urease inhibitors with potential applications in various fields, such as medicine or agriculture. For enhanced comprehension, figure-5 illustrates a bar chart depicting the urease inhibition activity of the precursor molecule, hydrazone ligand, and metal complexes. Figure 4 depicts a bar graph illustrating the comparative analysis between the ligand and metal complexes.

Figure 4: Comparative Urease Inhibitory Activity of Ligand and Metal Complexes

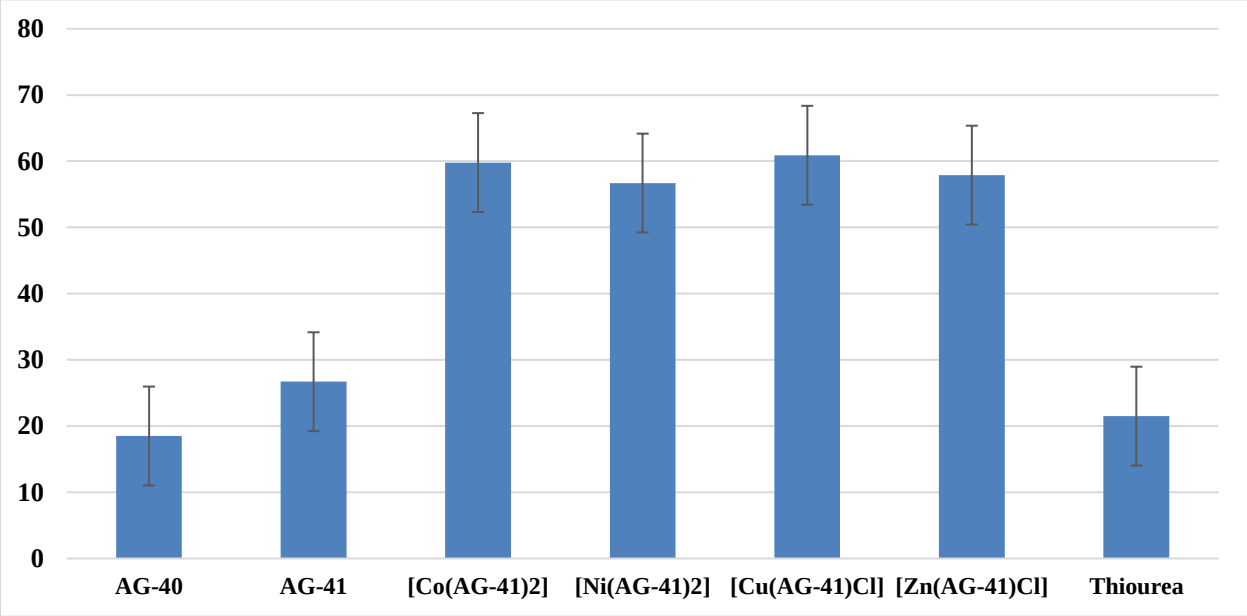

4 Conclusion

In this investigation, four novel complexes were synthesized using a hydrazone ligand denoted as AG-41, derived from 2-hydroxybenzaldehyde-N-(6-chloro-2-oxo-1,2-dihydro-3H-indol-3-ylidene). The complexes were formed with Co(II), Ni(II), Cu(II), and Zn(II), and underwent thorough characterization before being evaluated for their urease inhibition activities. It was observed that in all cases, the ligand AG-41 exhibited tridentate coordination with the metal center. Regarding urease inhibition, the metal complexes demonstrated a moderate potency, though they

were found to be less effective compared to the hydrazone ligand. Notably, both the ligand AG-41 and its precursor AG-40 exhibited excellent inhibitory properties when compared to the standard molecule, Thiourea.

5 Acknowledgement

We acknowledge for financial support from the Higher Education Commission of Pakistan under the national research grants program for universities (Grant No. 1463/R&D/09).

6 References

1. Campos, K. R., Coleman, P. J., Alvarez, J. C., Dreher, S. D., Garbaccio, R. M., Terrett, N. K., Tillyer, R.D., Truppo, M.D., & Parmee, E. R. (2019). The importance of synthetic chemistry in the pharmaceutical industry. *Science*, *363*(6424), eaat0805.
2. Kosikowska, P., & Berlicki, L. (2011). Urease inhibitors as potential drugs for gastric and urinary tract infections: a patent review. *Expert opinion on therapeutic patents*, *21*(6), 945-957. https://doi.org/10.1517/13543776.2011.574615
3. Qin, Y., & Cabral, J. M. (2002). Review properties and applications of urease. *Biocatalysis and biotransformation*, *20*(1), 1-14.
4. McLean, R. J., Nickel, J. C., Cheng, K. J., Costerton, J. W., & Banwell, J. G. (1988). The ecology and pathogenicity of urease-producing bacteria in the urinary tract. *CRC Critical reviews in microbiology*, *16*(1), 37-79.
5. Krajewska, B. (2018). Urease-aided calcium carbonate mineralization for engineering applications: A review. *Journal of Advanced Research*, *13*, 59-67.
6. Scott, D. R., Marcus, E. A., Weeks, D. L., & Sachs, G. (2002). Mechanisms of acid resistance due to the urease system of Helicobacter pylori. *Gastroenterology*, *123*(1), 187-195. https://doi.org/10.1053/gast.2002.34218
7. Jabeen, M. (2022). A comprehensive review on analytical applications of hydrazone derivatives. *Journal of the Turkish Chemical Society Section A: Chemistry*, *9*(3), 663-698. https://doi.org/10.18596/jotcsa.1020357
8. de Oliveira Carneiro Brum, J., França, T. C., LaPlante, S. R., & Villar, J. D. F. (2020). Synthesis and biological activity of hydrazones and derivatives: A review. *Mini reviews in medicinal chemistry*, *20*(5), 342-368. https://doi.org/10.2174/1389557519666191014142448
9. El-Sherif, A. A., & Aljahdali, M. S. (2013). Protonation, complex-formation equilibria, and metal–ligand interaction of salicylaldehyde Schiff bases. *Journal of Coordination Chemistry*, *66*(19), 3423-3468. https://doi.org/10.1080/00958972.2013.839027
10. Kolcu, F., Erdener, D., & Kaya, İ. (2020). A Schiff base based on triphenylamine and thiophene moieties as a fluorescent sensor for Cr (III) ions: Synthesis, characterization and fluorescent applications. *Inorganica Chimica Acta*, *509*, 119676. https://doi.org/10.1016/j.ica.2020.119676
11. Habala, L., Devínsky, F., & Egger, A. E. (2018). Metal complexes as urease inhibitors. *Journal of coordination chemistry*, *71*(7), 907-940. https://doi.org/10.1080/00958972.2018.1458228
12. Mohanan, K., & Murukan, B. (2005). Complexes of manganese (II), iron (II), cobalt (II), nickel (II), copper (II), and zinc (II) with a bishydrazone. *Synthesis and Reactivity in*

Inorganic, Metal-Organic, and Nano-Metal Chemistry, *35*(10), 837-844. http://dx.doi.org/10.1080/15533170500357988

13. Murukan, B., & Mohanan, K. (2006). Studies on some trivalent transition metal complexes with a bishydrazone. *Journal of Saudi Chemical Society*, *10*(2), 261-270.
14. Murukan, B., Sindhu Kumari, B., & Mohanan, K. (2007). Synthesis, spectral, electrochemical and antibacterial studies of copper (II) complexes with isatin derived bishydrazone and different co-ligands. *Journal of Coordination Chemistry*, *60*(15), 1607-1617.
15. Mazzei, L., Musiani, F., & Ciurli, S. (2020). The structure-based reaction mechanism of urease, a nickel dependent enzyme: Tale of a long debate. *JBIC Journal of Biological Inorganic Chemistry*, *25*(6), 829-845.
16. Murukan, B., & Mohanan, K. (2007). Synthesis, characterization and antibacterial properties of some trivalent metal complexes with [(2-hydroxy-1-naphthaldehyde)-3-isatin]-bishydrazone. *Journal of Enzyme Inhibition and Medicinal Chemistry*, *22*(1), 65-70. http://dx.doi.org/10.1080/14756360601027373
17. Arora, T., Devi, J., Boora, A., Taxak, B., & Rani, S. (2023). Synthesis and characterization of hydrazones and their transition metal complexes: antimicrobial, antituberculosis and antioxidant activity. *Research on Chemical Intermediates*, *49*(11), 4819-4843.
18. Tanoli, A. K., Khan, Z., Kamal, T., Ali, M., Latif, M., & Maqsood, Z. T. (2019). Metal-based biologically active compounds: Synthesis, spectral and antioxidant studies of transition metal complexes with hydrazone derivatives. *Pakistan Journal of Pharmaceutical Sciences*, *32*(1), 103-108.